

The effects of cannabidiol and its synergism with bortezomib in multiple myeloma cell lines. A role for transient receptor potential vanilloid type-2

Maria Beatrice Morelli^{1*}, Massimo Offidani^{2*}, Francesco Alesiani³, Giancarlo Discepoli⁴, Sonia Liberati⁵, Attilio Olivieri², Matteo Santoni¹, Giorgio Santoni¹, Pietro Leoni² and Massimo Nabissi¹

¹Section of Experimental Medicine, School of Pharmacy, University of Camerino, Camerino, Italy

²Clinica di Ematologia, Azienda Ospedaliero – Universitaria Ospedali Riuniti di Ancona, Ancona, Italy

³Unità di Oncoematologia, Ospedale di San Severino, San Severino Marche, Italy

⁴Laboratorio di Genetica Medica, Clinica di Pediatria, Ospedali Riuniti di Ancona, Ancona, Italy

⁵Department of Molecular Medicine, Sapienza University, Rome, Italy

Multiple myeloma (MM) is a plasma cell (PC) malignancy characterised by the accumulation of a monoclonal PC population in the bone marrow (BM). Cannabidiol (CBD) is a non-psychoactive cannabinoid with antitumoural activities, and the transient receptor potential vanilloid type-2 (TRPV2) channel has been reported as a potential CBD receptor. TRPV2 activation by CBD decreases proliferation and increases susceptibility to drug-induced cell death in human cancer cells. However, no functional role has been ascribed to CBD and TRPV2 in MM. In this study, we identified the presence of heterogeneous CD138+TRPV2+ and CD138+TRPV2- PC populations in MM patients, whereas only the CD138+ TRPV2- population was present in RPMI8226 and U266 MM cell lines. Because bortezomib (BORT) is commonly used in MM treatment, we investigated the effects of CBD and BORT in CD138+TRPV2- MM cells and in MM cell lines transfected with TRPV2 (CD138+TRPV2+). These results showed that CBD by itself or in synergy with BORT strongly inhibited growth, arrested cell cycle progression and induced MM cells death by regulating the ERK, AKT and NF- κ B pathways with major effects in TRPV2+ cells. These data provide a rationale for using CBD to increase the activity of proteasome inhibitors in MM.

Multiple myeloma (MM) is a haematological B cell malignancy characterised by clonal proliferation of plasma cells (PCs) and their accumulation in the bone marrow (BM).¹ MM displays enormous genomic instability and marked variation in clinical characteristics and patient survival.¹ In recent years, immunomodulatory drugs, proteasome inhibitors and other specific therapies have been developed to target myeloma cells and/or the BM microenvironment.² In addition, a number of new inhibitory agents targeting farnesyl-transferase, mitogen-activated protein kinases (MAPKs), pro-

tein kinase B (AKT) and cell cycle proteins (*e.g.*, cyclin D1 and D2) are currently under investigation for the treatment of relapsed/refractory MM in preclinical and clinical studies.³ Bortezomib (BORT), a 26S proteasome inhibitor, is used to treat relapsed and refractory MM patients, but the molecular mechanisms responsible for the favourable outcome of this treatment remain unclear.^{4,5} Although the initial overall rate of response to BORT is promising, the vast majority of patients who respond to this therapy develop resistance over time.^{1,2}

Key words: multiple myeloma, cannabidiol, transient receptor potential vanilloid type 2, bortezomib

Abbreviations: Abs: antibodies; AKT: protein kinase B; BM: bone marrow; BORT: bortezomib; BrdU: 5-bromo-2-deoxyuridine; CBD: cannabidiol; $\Delta\psi_m$: mitochondrial transmembrane potential; ERK: extracellular signal-related kinase; FACS: fluorescence activated cell sorting; FBS: foetal bovine serum; FISH: fluorescence *in situ* hybridisation; GAPDH: glyceraldehydes-3-phosphate dehydrogenase; MM: multiple myeloma; NAC: *N*-acetyl cysteine; pAKT: phospho protein kinase B; PC: plasma cell; pERK: phospho extracellular signal-related kinase; ROS: reactive oxygen species; RPMI_{TRPV2}: transient receptor potential vanilloid type 2-transfected RPMI cells; RR: ruthenium red; TRP: transient receptor potential cation channels; TRPV2: transient receptor potential vanilloid type 2; U266_{TRPV2}: transient receptor potential vanilloid type 2-transfected U266 cells.

Additional Supporting Information may be found in the online version of this article.

*M.B.M. and M.O. contributed equally to this work

Grant sponsor: AIL-Ancona ONLUS and the University of Camerino

DOI: 10.1002/ijc.28591

History: Received 21 Aug 2013; Accepted 22 Oct 2013; Online 8 Nov 2013

Correspondence to: Massimo Nabissi, University of Camerino, Section of Experimental Medicine, School of Pharmacy, via Madonna delle Carceri 6, 62032 Camerino (MC), Italy, Tel.: +3-907-3740-3306/12/37, Fax: +3907-3740-3325, E-mail: massimo.nabissi@unicam.it

What's new?

Cannabidiol, a non-psychoactive component of Cannabis, has antitumor properties. This study investigated whether cannabidiol could assist another drug, bortezomib, in fighting multiple myeloma. Although patients respond well to bortezomib at first, most develop resistance to it over time. The authors looked in myeloma cell lines and patient samples for a protein, TRPV2, which interacts with cannabidiol. They found that cannabidiol, working alone or in concert with bortezomib, kills multiple myeloma cells, particularly when TRPV2 was expressed. These data suggest that treatment with cannabidiol may help sidestep the problem of patients developing resistance to bortezomib.

MM cells exhibit mutations in the nuclear factor kappa-light-chain-enhancer of activated B cells [NF- κ B] pathway, and this family of transcription factors, including NFKB1 (p50), NFKB2 (p52), RelA (p65), RelB and c-Rel, is involved in the canonical and alternative pathways regulating MM proliferation, survival and chemoresistance.^{6,7} The canonical RelA/p50 pathway is predominantly regulated by I κ B α , a substrate of the proteasome, which rationalises the use of BORT in the treatment of MM because this drug can inhibit I κ B α . However, it is not clear whether BORT-induced cytotoxicity is entirely due to its inhibition of the canonical NF- κ B pathway.^{8–10} Unfortunately, the clinical activity of a single agent is limited, although the therapeutic efficacy can be enhanced by combining a single drug with conventional agents and/or steroids.¹¹ Nonetheless, new approaches are needed to improve the activity of proteasome inhibitors.

More recently, subgroups of MM have been defined in terms of genetic and cytogenetic abnormalities. Fluorescence *in situ* hybridisation (FISH) analysis on sorted CD138⁺ PCs can detect abnormalities such as t(4:14), t(14:16) or loss of 17p, which are associated with a poor outcome, whereas MM patients harbouring hyperdiploidy and t(11;14) translocation generally have better prognoses.¹² The human *transient receptor potential vanilloid type-2 (TRPV2)* gene, located on chromosome 17p11.2, encodes nonselective Ca²⁺ channels. It is structurally composed of six transmembrane domains, a putative pore-loop region, a cytoplasmic amino terminus with three ankyrin-repeat domains and a cytoplasmic carboxyl terminus.

TRPV2 belongs to the family of transient receptor potential (TRP) cation channels,¹³ which is involved in the regulation of tumour growth, progression, invasion and angiogenesis.^{14,15} Previously, we demonstrated that *TRPV2* overexpression was correlated with a decrease in proliferation and an increase in drug-uptake and chemosensitivity *via* a mechanism involving the inhibition of the Ras/Raf/MEK/ERK pathway in human glioblastomas.^{16–18} Moreover, TRPV2 has also been shown to promote brain cancer stem-like cell differentiation.¹⁸ *TRPV2* gene mutations (gain or loss of function) have been identified in haematological disorders such as MM,^{19,20} and a 5-Mb 17p11.2-p12 amplified region was detected in KMS-26 myeloma cells by SNP analysis.²⁰ However, to date, no functional role has been ascribed to TRPV2 in MM.

Functional studies on the TRPV2 channels in glioma cell lines have revealed that agonists such as cannabidiol (CBD)

trigger TRPV2 activation, thereby increasing drug uptake and cytotoxicity.¹⁷ CBD is a cannabinoid component from *Cannabis sativa* that demonstrates affinity for cannabinoid (CB1 and CB2) receptors, vanilloid receptors (*e.g.*, TRPV1, TRPV2) and peroxisome proliferator-activated receptor gamma (PPAR γ)^{21–23} In addition, CBD possesses anti-inflammatory and immunomodulatory properties but does not induce psychotomimetic effects.²⁴

In vitro and *in vivo* studies have shown that CBD promotes antitumoural effects by increasing cell death and reducing the proliferation, invasion, and migration of different mammalian cancer cells in a CB1- and CB2-dependent and -independent manner.^{17,18,25,26} The aim of this study was to evaluate the expression of TRPV2 in MM cell lines and PCs obtained from newly diagnosed MM patients as well as the TRPV2-dependent and -independent effects of CBD alone and in combination with BORT, in MM cell lines.

Material and Methods**Cells**

RPMI8226 (RPMI) and U266 MM cell lines were purchased from ATCC (LGC Standards, Milan, IT). Cell authentication was performed by IST (Genova, Italy). Briefly, short tandem repeat [STR] profile has been carried out on RPMI and U266 cell lines. Nine highly polymorphic STR loci plus amelogenin (Cell IDTM System, Promega, WI) were used. Detection of amplified fragments was obtained by ABI PRISM 3100 Genetic Analyser (Paisley, UK). Data analysis was performed by GeneMapper software, version 4.0. Cell lines were cultured in RPMI medium (Lonza, Milan, IT) supplemented with 10% foetal bovine serum (FBS), 2 mM L-glutamine, 100 IU/ml penicillin, 100 μ g streptomycin and 1 mM sodium pyruvate. Cell lines were maintained at 37°C with 5% CO₂ and 95% humidity. Freshly isolated CD138⁺ PCs from BM aspirates were obtained from newly diagnosed MM patients. Informed consent was provided for a protocol approved by the Polytechnic University of the Marche (study n CLEM 01-09), in accordance with the Declaration of Helsinki. CD138⁺ PCs were isolated using the EasySep Human CD138 Positive Selection kit (Stem Cell Technologies, Vancouver, Canada). Whole blood from healthy donors was used to isolate CD34⁺ haematopoietic progenitors using the CD34 MicroBead kit (StemCell Technologies). CD138⁺ and CD34⁺ purity was determined by flow cytometry analysis.

Antibodies

The following mouse monoclonal antibodies (Abs) were used: phycoerythrin [PE]-conjugated anti-human CD138 (20 μ l/sample), PE-conjugated IgG1 κ isotype control (20 μ l/sample), PE conjugated anti-human CD34 (20 μ l/sample) (all purchased from BD Biosciences, San Jose, CA); anti-phospho extracellular signal-related kinase [pERK] (1:2,000) (Cell Signalling Technology, Danvers, MA) and anti-GAPDH-peroxidase (1:5,000) (Sigma-Aldrich, St. Louis, MO). The following polyclonal Abs were used: goat anti-TRPV2 (1:50 for fluorescence activated cell sorting [FACS] analysis, 1:200 for Western blot analysis), normal goat IgG (1:200), FITC-conjugated donkey anti-goat (1:20), rabbit anti-cyclin D1 (1:200), horseradish peroxidase (HRP)-conjugated donkey anti-goat IgG (1:1,000) (all purchased from Santa Cruz Biotechnology, Santa Cruz, CA); rabbit anti-phospho protein kinase B (pAKT; 1:1,000) and rabbit anti-ERK (1:1,000) (Cell Signalling Technology); rabbit anti-AKT (1:1,000) (Signalway Antibody, Pearland, TX) and HRP-conjugated donkey anti-rabbit IgG (1:2,000) (GE Healthcare, Munich, Germany).

Compounds

CBD, Ruthenium Red (RR), AM251, AM630 and GW9662 were purchased from Tocris Bioscience (Bristol, UK), and 25 mM aliquots were prepared (CBD, AM251, AM630 and GW9662 in dimethyl sulphoxide [DMSO], RR in water). *N*-Acetyl cysteine (NAC) was purchased from Sigma-Aldrich and 0.5 M aliquots were prepared. BORT was provided by Janssen-Cilag International N.V. (Beerse, Belgium), and 1 μ g/ml aliquots were prepared in water.

FISH analysis

FISH analysis using Vysis Locus Specific Identifier probes was performed as recommended by the manufacturer (Vysis, Inc., Downers Grove, IL). The following probes were used to analyse the structure of chromosome 17p: LIS1 in 17p13.3, *p53* in 17p13.1 and proteasome Magenis syndrome (SMS) in 17p11.2. The control probes were D17Z1 in 17p10q10 (centromere 17) and RAR-A in 17q22. Slides were examined using a Zeiss Axioplan 2 (Carl Zeiss AG, Göttingen, Germany) epifluorescent microscope with single and dual band-pass filter sets for the visualisation of spectrum green, orange and 4',6-diamidino-2-phenylindole [DAPI] fluorescence. Images were captured and enhanced using a photometrics image point CCD camera coupled with MacProbe 4.0 software. In each sample, the number of locus-specific signals was evaluated for interphase nuclei.

FACS analysis

The expression of CD138, CD34 and TRPV2 was determined using PE-conjugated anti-CD138, PE-conjugated anti-CD34, anti-TRPV2 and FITC-conjugated anti-goat Abs. Briefly, cells were fixed with 4% paraformaldehyde and incubated with the primary or isotype-specific Abs. The cells were then washed

with staining buffer (phosphate-buffered saline [PBS], 1% FBS and 0.1% NaN_3) and permeabilisation buffer (PBS, 1% FBS, 0.1% NaN_3 and 1% saponin) and incubated with anti-TRPV2 or normal goat IgG (negative control). The pellets were then incubated with FITC-conjugated anti-goat Abs and analysed using a FACScan cytofluorimeter (BD Bioscience) with CellQuest software (BD Pharmingen, Milan, IT).

Cell transfection

RPMI and U266 cells were plated at a density of 3×10^4 per cm^2 , and after overnight incubation, 1 μ g/ml of pCMV_{TRPV2} or pCMV_{empty} (empty vector) were added to the wells according to the METAFECTENE EASY protocol (Biontex Laboratories, San Diego, CA). The cells were harvested at day 3 post-transfection for analysis. The efficiency of transfection was evaluated by Western blot and flow cytometry analysis. Only transfected cells (*transient receptor potential vanilloid type 2*-transfected RPMI cells [RPMI_{TRPV2}] and transient receptor potential vanilloid type 2-transfected U266 cells [U266_{TRPV2}]) with 70% or more TRPV2⁺ cells were used for the experiments.

Colony forming assay

Purified CD34⁺ cells were resuspended in Iscoves Modified Dulbecco's medium [MDM] (StemCell Technologies) supplemented with 2% FBS and treated with CBD and BORT alone or in combination. The cells were then diluted in MethoCult H4034 Optimum (StemCell Technologies) and dispensed in duplicate 35-mm culture plates, with 5×10^3 cells in each plate. Colonies were scored on day 12.

Gene expression analysis

Total RNA was isolated using the RNeasy Mini kit (Qiagen, Milan, IT). Complementary DNA (cDNA) was synthesised using the high-capacity cDNA archive kit (Life Technology, Milan, IT). Polymerase chain reaction (PCR) for *TRPV1*, *TRPV2*, *TRPV3* and *p53* was performed using specific primers and the following thermal cycling conditions: 5' at 95°C; 35 cycles of 10'' at 95°C, 20'' at 60°C, 30'' at 72°C; and finally 5' at 72°C (MyCycler instrument, Bio-Rad, Hercules, CA). PCR products were run on 1.5% agarose gels, and bands were detected using Sybr Green staining and Chemi-Doc (Bio-Rad) detection.

Western blot analysis

MM cells were lysed as described previously.¹⁷ Twenty micrograms of the lysate was separated on a SDS-polyacrylamide gel, transferred onto Hybond-C extra membranes (GE Healthcare), blocked with 5% low-fat dry milk in PBS-Tween 20, immunoblotted with TRPV2, pERK, ERK, pAKT, AKT, cyclin D1 and glyceraldehydes-3-phosphate dehydrogenase (GAPDH) Abs overnight and then incubated with HRP-conjugated Ab for 1 hr. Immunostaining was revealed using an enhanced chemiluminescence Western blotting analysis system (GE Healthcare). Densitometric

analysis was performed using ChemiDoc with Quantity One software (Bio-Rad).

3-[4,5-dimethylthiazol-2-yl]-2,5 diphenyl tetrazolium bromide [MTT] assay

Three thousand cells per well were seeded in 96-well plates. After 1 day of incubation, compounds or vehicles were added. Four replicates were used for each treatment. At the indicated time point, cell viability was assessed by adding 0.8 mg/ml of MTT (Sigma-Aldrich) to the media. After 3 hr, the plates were centrifuged, the supernatant was discharged, and the pellet was solubilised with 100 μ l/well DMSO. The absorbance of the samples against a background control (medium alone) was measured at 570 nm using an ELISA reader microliter plate (BioTek Instruments, Winooski, VT). In some experiments, preincubation (3 hr) with 10 mM NAC was performed. Synergistic activity of the CBD/BORT combination was determined by the isobologram and combination index (CI) methods (CompuSyn Software, ComboSyn, Inc. Paramus, NJ 2007). The CI was used to express synergism (CI < 1), additivity (CI = 1) or antagonism (CI > 1) and was calculated according to the standard isobologram equation.²⁷

BrdU cell proliferation assay

The incorporation of 5-bromo-2-deoxyuridine (BrdU) was assessed using the BrdU Cell Proliferation Assay (Millipore, Billerica, MA). Incorporated BrdU was detected by adding the peroxidase substrate. Spectrophotometric detection was performed at a dual wavelength of 450/550 nm using an ELISA reader microliter plate.

Cell cycle analysis

For this analysis, 3×10^5 cells/ml were incubated with the appropriate drugs for up to 72 hr. Cells were fixed for 1 hr by adding ice-cold 70% ethanol and then washed with staining buffer (PBS, 2% FBS and 0.01% NaN_3). Next, the cells were treated with 100 μ g/ml ribonuclease A solution (Sigma-Aldrich), incubated for 30 min at 37°C, stained for 30 min at room temperature with PI 20 μ g/ml (Sigma-Aldrich) and finally analysed by flow cytometry using linear amplification.

Apoptosis assays

The exposure of phosphatidylserine on MM cells was detected by Annexin V staining and cytofluorimetric analysis. Briefly, 2×10^4 cells were treated with different doses of the appropriate drugs for a maximum of 72 hr. Four replicates were used for each treatment. After treatment, the cells were stained with 5 μ l of Annexin V FITC (Vinci Biochem, Vinci, Italy) for 10 min at room temperature, washed once with binding buffer (10 mM N-(2-Hydroxyethyl)piperazine-N'-2-ethanesulfonic acid [HEPES]/sodium hydroxide, pH 7.4, 140 mM NaCl, 2.5 mM CaCl_2) and analysed on a FACScan flow cytometer using CellQuest software.

PI staining

After treatment with the appropriate drugs for a maximum of 72 hr, 2×10^4 MM cells were incubated in a binding

buffer containing 20 μ g/ml PI for 10 min at room temperature. The cells were then analysed by flow cytometry using CellQuest software.

Mitochondrial transmembrane potential

Mitochondrial transmembrane potential ($\Delta\psi_m$) was evaluated by 5,5',6,6'-tetrachloro-1,1',3,3'-tetraethylbenzimidazolylcarbocyanineiodide (JC-1) staining. Briefly, 2×10^4 cells were treated with the appropriate drugs for different times (up to 6 hr) and then incubated for 10 min at room temperature with 10 μ g/ml of JC-1. JC-1 was excited by an argon laser (488 nm), and the green (530 nm)/red (570 nm) emission fluorescence was collected simultaneously. Carbonyl cyanide chlorophenylhydrazone protonophore, a mitochondrial uncoupler that collapses ($\Delta\psi_m$), was used as a positive control (data not shown). Samples were analysed using a FACScan cytofluorimeter with CellQuest software.

ROS production

The fluorescent probe dichlorodihydrofluorescein diacetate (DCFDA) was used to assess oxidative stress levels. Briefly, 2×10^4 cells treated with the appropriate compounds were incubated with 20 μ M DCFDA (Life Technologies Italia, Italy) 20 min prior to the harvest time point. In some experiments, cells were preincubated for 3 hr with 10 mM NAC. The cells were then washed, and the intensity of the fluorescence was assayed using flow cytometry and CellQuest software.

DNA fragmentation assay

Electrophoresis of DNA extracts was performed to assess DNA fragmentation as a criterion for necrosis and apoptosis. Briefly, 1.5×10^6 cells were treated with the appropriate compounds for a maximum of 3 days, and genomic DNA was extracted using a DNA extraction kit (Qiagen). The purified samples were then subjected to electrophoresis on a 1.25% agarose gel, and DNA was stained with ethidium bromide. Ultraviolet spectroscopy at 302 nm was used to obtain the results.

NF- κ B DNA-binding activity

Activated p50, p65, p52 and RelB NF- κ B subunit proteins were quantified using the TransAm Flexi NF- κ B family transcription factor ELISA assay (Active Motif, La Hulpe, Belgium).

Statistical analysis

The data presented represent the mean and standard deviation (SD) of at least 3 independent experiments. The statistical significance was determined by analysis of variance or Student's *t*-test; *,[#],^S,^C *p* < 0.01. The statistical analysis of IC₅₀ levels was performed using Prism 5.0a (Graph Pad). Data from pCMV_{empty}-transfected RPMI and U266 cells were omitted because no effects were observed when compared with untransfected cells. No differences were found between

Table 1. Expression of TRPV2 in CD138+ PCs derived from MM patients¹

P	FISH	% Pathological cells	del17p	% CD138 ⁺ /TRPV2 ⁺	% CD138 ⁺ /TRPV2 ⁻
1	Hyperdiploid	25	–	44	56
2	t(11;14)	40	–	91	9
3	del 13	100	–	93	7
4	Hyperdiploid	20	–	70	30
5	Hyperdiploid	40	–	68	32
6	Hyperdiploid	35	–	40	60
7	t(11;14) Hypodiploid	50	–	56	44
8	Diploid	90	–	90	10
9	del 13	40	–	33	67
10	Diploid	3	–	33	67
11	t(11; 14)	90	–	9	91
12	Diploid	70	–	45	55
13	t(11; 14)	15	–	70	30

¹BM aspirates were collected from MM patients (P) ($n = 13$), and the percentage of pathological cells in aspirates was determined. All samples were also karyotyped by FISH to detect the 17p deletion (del17p). All samples were subjected to an enrichment procedure to increase CD138⁺ tumour cells by CD138⁺ cell sorting. The percentage of TRPV2⁺ and TRPV2⁻ cells among CD138⁺ purified PCs was evaluated using flow cytometry.

drug treatments in the untransfected *versus* pCMV_{empty}-transfected cells.

Results

Expression of TRPV2 and FISH analysis in CD138⁺ PCs from MM patients and in MM cell lines

The percentage of pathological cells was determined according to the PC counts of BM slides from 13 newly diagnosed patients. As shown, the percentages varied from approximately 3–100%. None of the samples analysed by FISH demonstrated the presence of del17p (Table 1). In all samples, flow cytometry analysis of TRPV2 expression on CD138⁺ enriched PCs demonstrated the presence of two distinct CD138⁺ PC subpopulations based on the expression of TRPV2 (CD138⁺ TRPV2⁺ and CD138⁺ TRPV2⁻; Table 1; Supporting Information Figs. S1a and S1b). Then, we performed cytogenetic analysis to investigate TRPV2 in the RPMI and U266 MM cell lines. By FISH analysis, we found tetraploid RPMI cells with a short deletion of two 17p arms and diploid U266 cells showing a large deletion of one 17p phenotype (Supporting Information Table S1). By flow cytometry and Western blot analysis, we found that both MM cell lines were CD138⁺TRPV2⁻ (Fig. 1a; Supporting Information Figs. S1c and S1d), resembling the CD138⁺TRPV2⁻ subpopulation identified in MM patients. PCR analysis of total RNA extracted from RPMI and U266 cells showed that genes such as *TRPV1*, *TRPV2*, *TRPV3* and *p53* that were localised in the 17p region were not expressed (Supporting Information Fig. S2). Furthermore, transfection of RPMI and U266 cells with a plasmid expressing h-*TRPV2* gave rise to MM cells with a CD138⁺TRPV2⁺ phenotype, as evaluated by flow cytometry and Western blot analyses (Fig. 1a; Supporting Information Figs. S1c and S1d).

TRPV2 expression increases CBD-induced cytotoxicity in MM cell lines

The effects of CBD were evaluated in *TRPV2*-transfected and untransfected cells. We found that the RPMI_{TRPV2} and U266_{TRPV2} cell lines were more susceptible to the effects of CBD in a time- and dose-dependent manner compared with untransfected MM cells (IC₅₀ at day 3: RPMI 22.4 μM, RPMI_{TRPV2} 13.5 μM, U266 32.2 μM, U266_{TRPV2} 19.8 μM), demonstrating that TRPV2 expression reduced the IC₅₀ in CBD-treated transfected-MM cells by approximately 40% (Figs. 1b and 1c; Supporting Information Fig. S3). To further evaluate the selectivity of CBD for TRPV2, TRPV2-transfected and untransfected MM cell lines were treated with 20 μM of AM251 (CB1 selective antagonist), 20 μM AM630 (CB2 selective antagonist), 12.5 μM GW9662 (selective PPARγ antagonist) or 10 μM RR (TRP channel blocker); these drugs were administered alone or in combination with the lowest effective dose of CBD (20 μM), which demonstrated an inhibition rate of 25% in RPMI cells and 24% in U266 cells at day 3 post-treatment. As shown by MTT assay, the AM251, AM630, GW9662 and RR treatments did not revert the effect of CBD on cell viability in RPMI and U266 cells (Figs. 1d and 1e), whereas RR markedly reverted the TRPV2-dependent CBD-induced effects in RPMI_{TRPV2} and U266_{TRPV2} cells (Figs. 1f and 1g).

BORT and CBD synergise to increase cytotoxicity in MM cell lines

We performed time-course (up to 3 incubation days) and dose-response (BORT 1 to 25 ng/ml) experiments in RPMI and U266 cell lines (IC₅₀ at day 3: RPMI = 3.24 ng/ml, RPMI_{TRPV2} = 2.98 ng/ml, U266 = 4.36 ng/ml; U266_{TRPV2} =

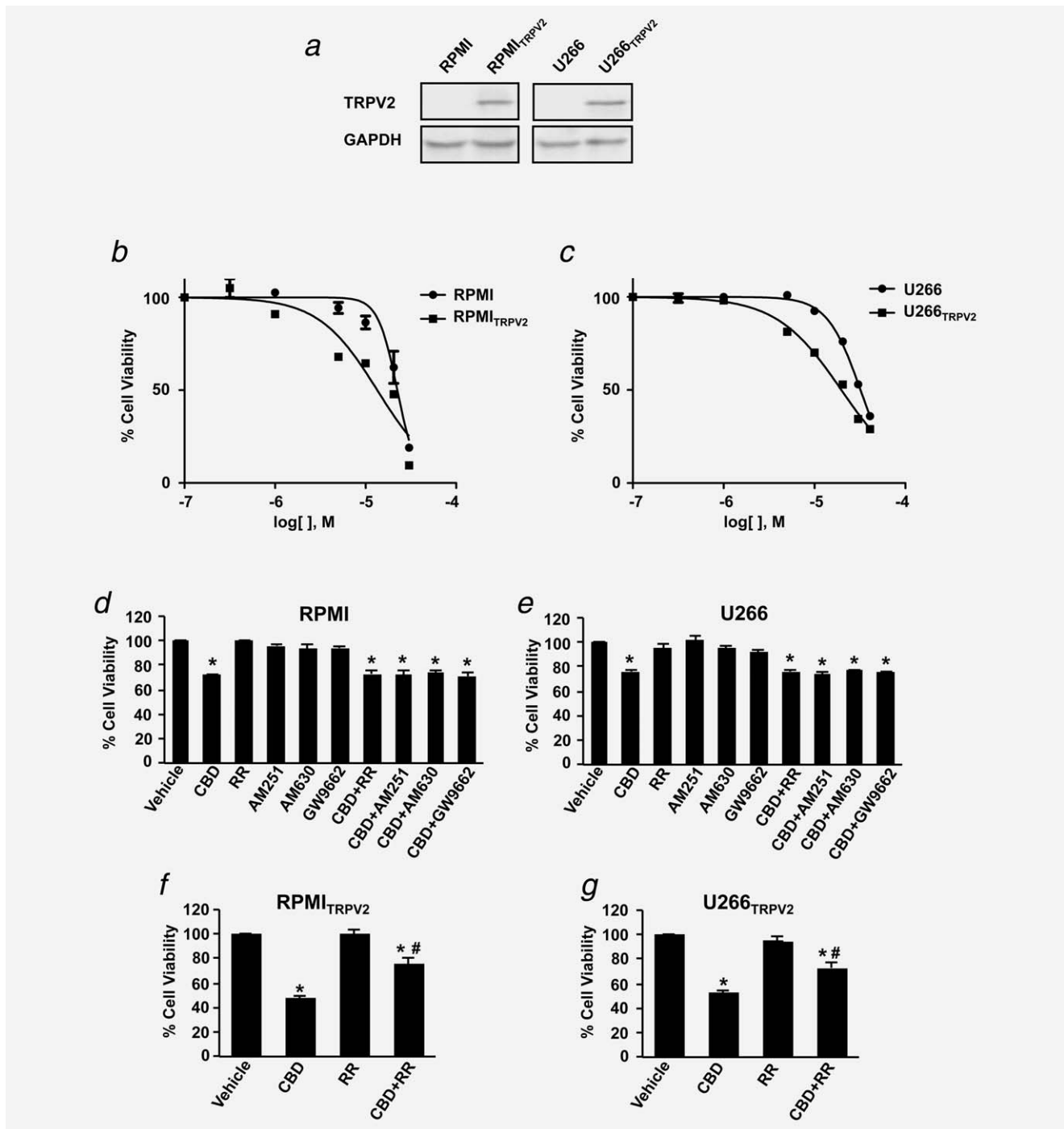


Figure 1. Expression of TRPV2 and TRPV2 dependent and independent induced CBD cytotoxicity in RPMI and U266 MM cell lines. (a) Representative analysis of TRPV2 protein expression (MW 86 kDa) in RPMI, RPMI_{TRPV2}, U266 and U266_{TRPV2} cells evaluated by Western blot analysis. Lysates were immunoblotted with anti-TRPV2 Ab. GAPDH protein levels were used as loading control. Blots are representative of one of three separate experiments. (b,c) Transfected and untransfected MM cell lines were cultured for 3 days with different doses of CBD. Cell viability was determined by MTT assay. Data shown are expressed as mean ± standard error of three separate experiments. (d–g) RPMI, U266, RPMI_{TRPV2} and U266_{TRPV2} cells were treated for 3 days with CBD (20 μM) alone and in combination with RR (10 μM), AM251 (20 μM), AM630 (20 μM) or GW9662 (12.5 μM). The percentage of viable cells was determined by MTT assay. Data shown are the mean ± SD of at least three separate experiments. **p* < 0.01 vs. vehicle; #*p* < 0.01 CBD + RR vs. CBD or RR.

4.07 ng/ml; *p* < 0.01). We found that treatment with 3 ng/ml of BORT was the lowest effective dose that reduced the viability of both transfected and untransfected MM cell lines

(percentage of inhibition: RPMI = 44, RPMI_{TRPV2} = 48, U266 = 38, U266_{TRPV2} = 37) at day 3 of treatment (Figs. 2a–2d). Furthermore, the coadministration of 20 μM CBD

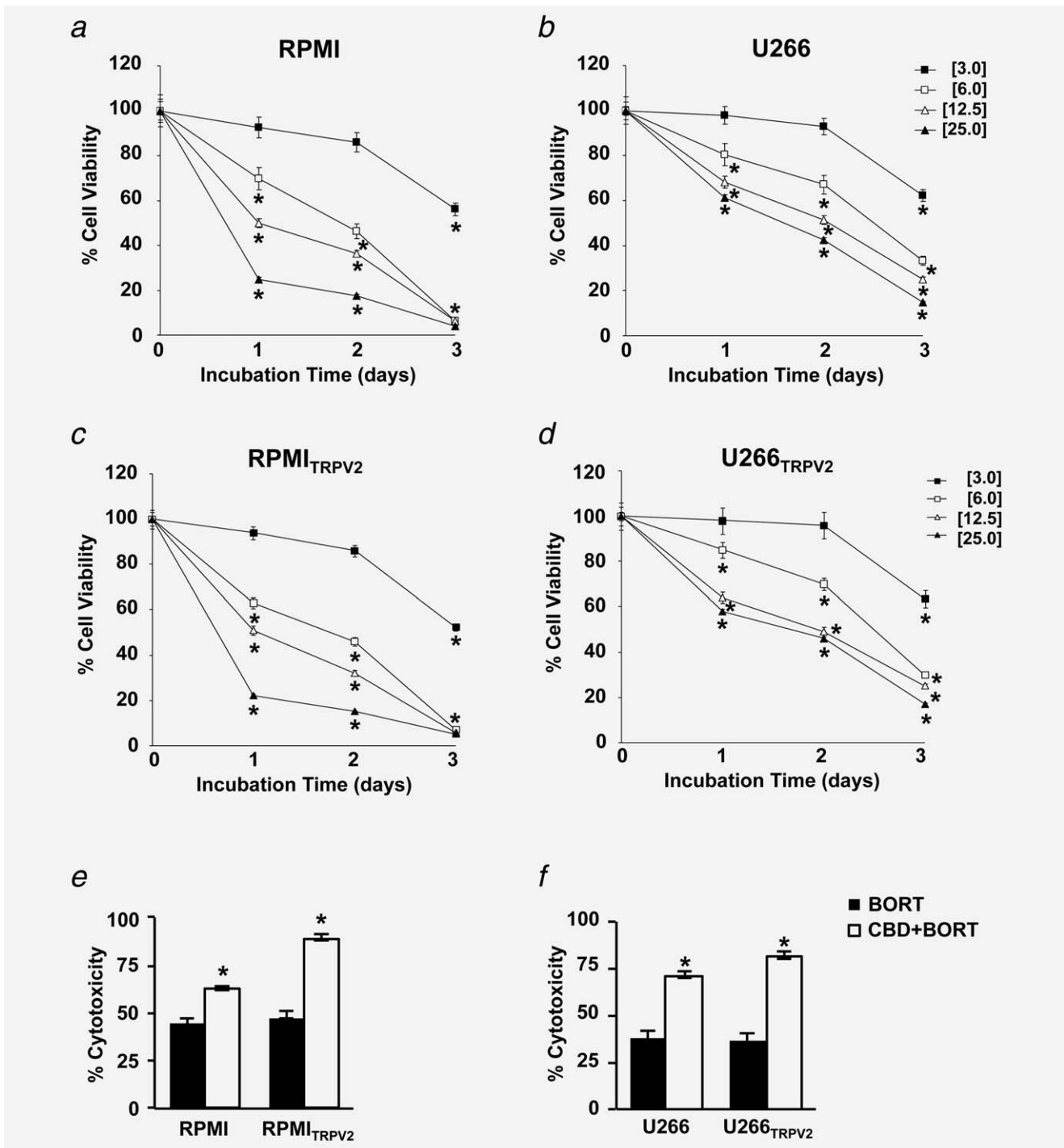


Figure 2. TRPV2 triggers the synergistic cytotoxic effect of CBD and BORT on MM cell lines (*a–d*) RPMI, U266, RPMI_{TRPV2} and U266_{TRPV2} cell lines were cultured for a maximum of 3 days in the presence of BORT (3–25 ng/ml). The percentage of viable cells was determined by MTT assay. The data are represented as the mean \pm SD of at least three separate experiments. * $p < 0.01$ BORT vs. vehicle. (*e–f*) MM cell lines were cultured for 3 days in the presence of CBD (20 μ M) and BORT (3 ng/ml) alone or in combination. Cell viability was determined by MTT assay. The data are represented as the mean \pm SD of at least three separate experiments. * $p < 0.01$ CBD-BORT vs. BORT.

and 3 ng/ml of BORT acted synergistically to inhibit the viability of MM cells (CI < 1; Figs. 2*e* and 2*f*; Supporting Information Table S2 and Fig. S4). So, CBD added in BORT treatment strongly enhances BORT effect, observing a

response comparable to that obtained by the use of higher BORT doses, in both cell lines. In addition, the cytotoxic effect of CBD alone or in combination with BORT was evaluated in CD34⁺ cells isolated from healthy blood donors

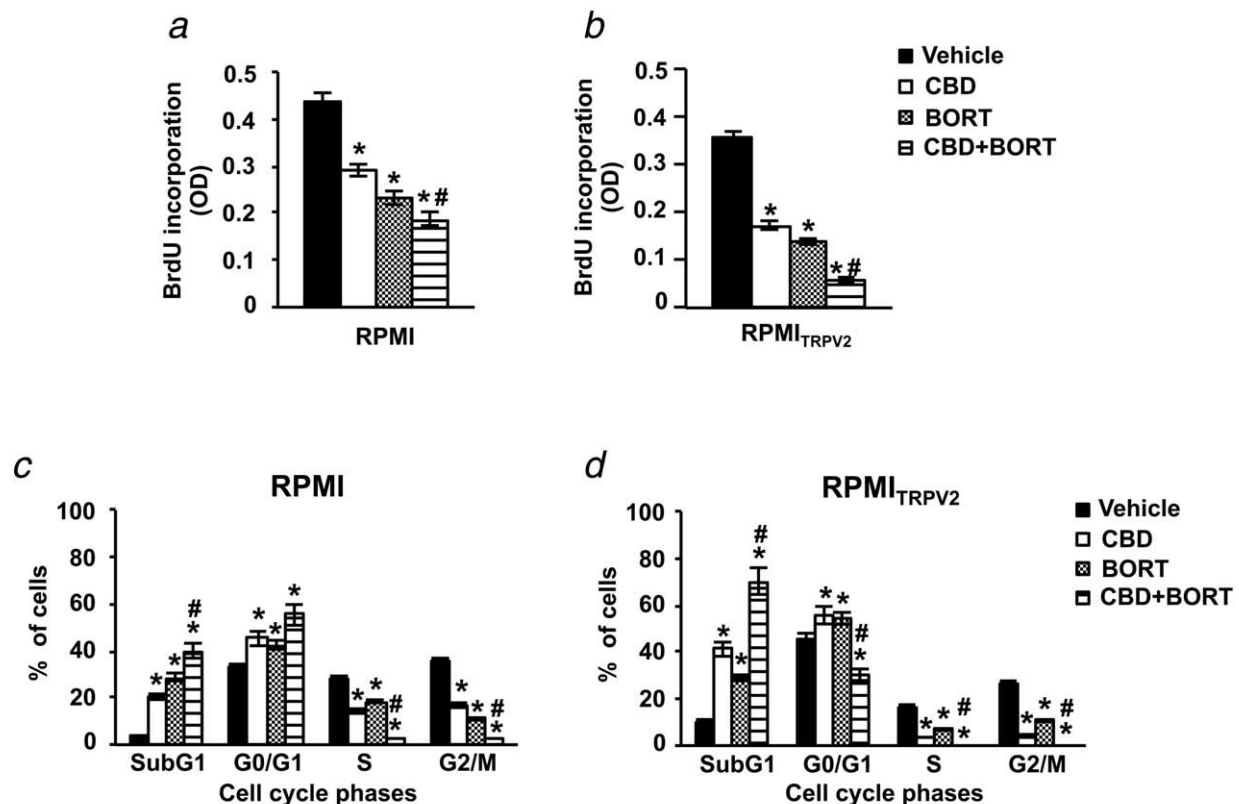


Figure 3. TRPV2 triggers a CBD-mediated reduction in proliferation and cell cycle regulation in RPMI and RPMI_{TRPV2} cells. RPMI and RPMI_{TRPV2} cells were cultured for 3 days in the presence of CBD (20 μ M) and BORT (3 ng/ml) alone or in combination. (a,b) Proliferation was assessed with the BrdU incorporation assay. The values of BrdU incorporation were reported in terms of OD. (c,d) MM cells were stained with PI solution to assess the cell cycle distribution pattern. The values were expressed as the percentage of cells in each phase. The data are represented as the mean \pm SD of at least three separate experiments. * $p < 0.01$ vs. vehicle; # $p < 0.01$ CBD-BORT vs. CBD or BORT alone.

expressing low TRPV2 levels (Supporting Information Fig. S5A). Colony forming assays (CFU-GM) demonstrated that the growth of CD34⁺ cells was unaffected by this combination of drugs (Supporting Information Fig. S5B).

BORT and CBD inhibit proliferation by inducing cell cycle arrest in MM cell lines

By performing a BrdU incorporation assay, the effects of CBD and BORT alone and in combination were evaluated at day 3 after treatment in RPMI, U266, RPMI_{TRPV2} and U266_{TRPV2} cells. CBD or BORT treatment reduced the proliferation in both MM cell lines, with the major effects observed in TRPV2-transfected compared with untransfected cells (Figs. 3a and 3b; Supporting Information Figs. S6a and S6b). Moreover, CBD and BORT coadministration strongly reduced proliferation, mainly in TRPV2-transfected cells compared with untransfected cells (Figs. 3a and 3b; Supporting Information Figs. S6a and S6b). In addition, the effects of CBD and BORT on cell cycle progression were analysed. The results showed that CBD and BORT arrested the cell cycle at the G1 phase and induced cell accumulation in the sub-diploid (sub-G1) phase, with stronger effects observed in BORT plus CBD-treated cells compared with vehicle-treated

cells (Figs. 3c and 3d; Supporting Information Figs. S6c and S6d). In TRPV2-transfected cells, CBD or BORT increased the percentage of cells in the sub-G1 and G1 phases compared with untransfected cells (Figs. 3c and 3d; Supporting Information Figs. S6c and S6d). Moreover, CBD and BORT strongly increased frequency of TRPV2-transfected cells in the sub-G1 phase as compared with untransfected cells (70% in RPMI_{TRPV2} vs. 40% in RPMI; 70% in U266_{TRPV2} vs. 38% in U266; $p < 0.01$; Figs. 3c and 3d; Supporting Information Fig. S6c and S6d).

BORT and CBD induce mitochondrial and ROS-dependent necrosis in MM cell lines

CBD and BORT markedly increased the percentage of PI⁺/Annexin V⁻ necrotic MM cells and the intensity of DNA fragmentation in TRPV2-transfected cell lines compared with untransfected cells (Figs. 4a and 4b; Supporting Information Figs. S7a and S7b). In addition, a slight increase in PI⁺ necrotic cells and DNA fragmentation was found both in untransfected and transfected MM cells treated with CBD (RPMI = 52, RPMI_{TRPV2} = 65, U266 = 66, U266_{TRPV2} = 88; $p < 0.01$) or BORT (RPMI = 72, RPMI_{TRPV2} = 71, U266 = 57, U266_{TRPV2} = 66; $p < 0.01$) alone, whereas this

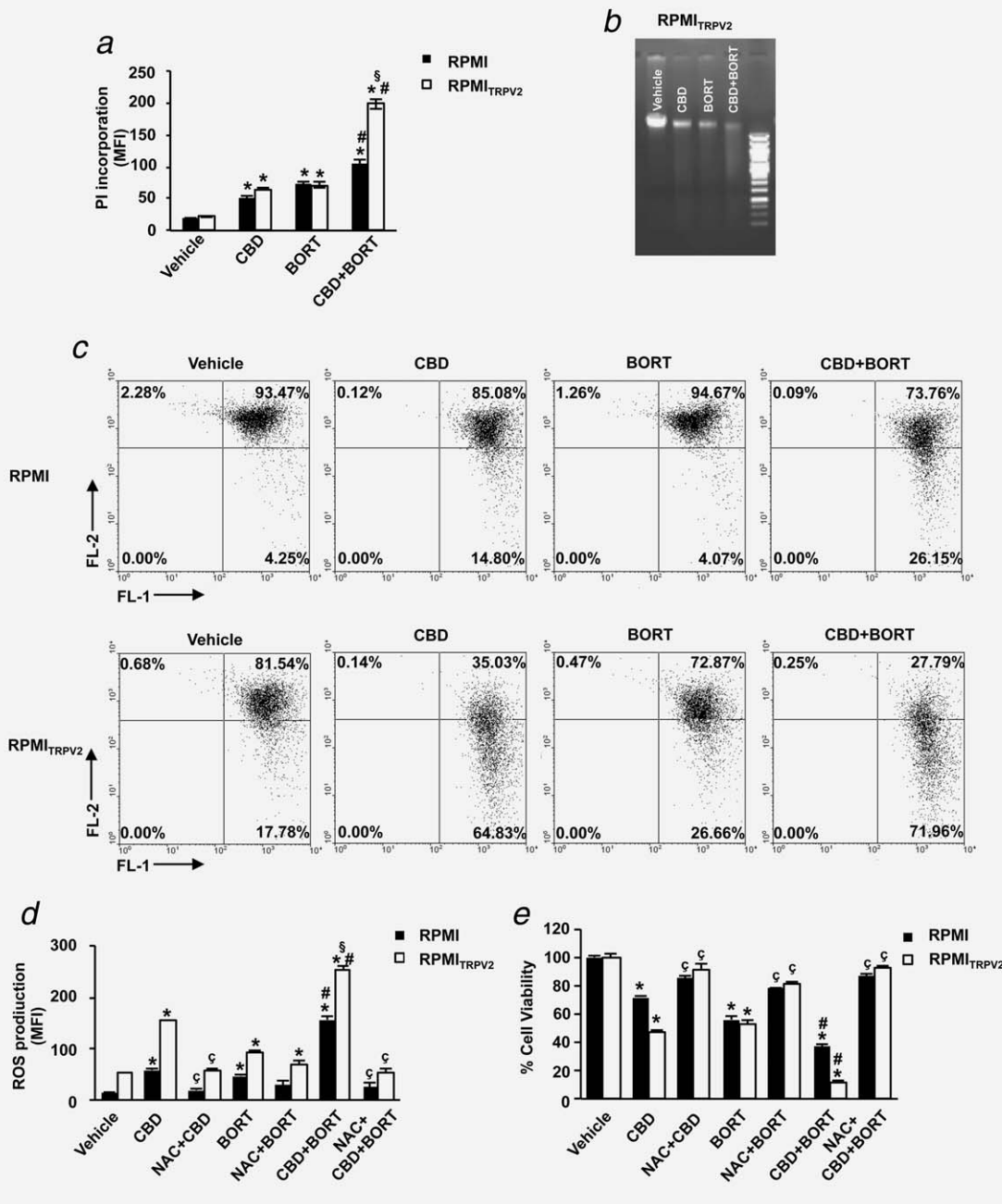


Figure 4. TRPV2 increases CBD and BORT combination therapy-induced necrosis in RPMI and RPMI_{TRPV2} cells. RPMI and RPMI_{TRPV2} cells were cultured in the presence of CBD (20 μ M) and BORT (3 ng/ml) alone or in combination. (a) Cells treated for 3 days were permeabilised, stained with PI and then assessed for fluorescence by flow cytometry. The data are represented as the mean fluorescence intensity \pm SD of at least three separate experiments. * p < 0.01 vs vehicle; # p < 0.01 CBD-BORT vs CBD or BORT alone; \S p < 0.01 TRPV2-transfected vs. untransfected cell lines. (b) Representative agarose gel electrophoresis of DNA extracts obtained from RPMI_{TRPV2}-treated cells at day 3 for the assessment of DNA fragmentation. (c) RPMI and RPMI_{TRPV2} cells were treated with CBD (20 μ M) and BORT (3 ng/ml) alone or in combination for 1 hr. Changes in $\Delta\Psi_m$ were evaluated by JC-1 staining and biparametric FL1(green)/FL2(red) flow cytometric analysis. Numbers indicate the percentage of cells showing a drop in the $\Delta\Psi_m$ -related red fluorescence intensity. The data are representative of at least three independent experiments. (d) RPMI and RPMI_{TRPV2} cell lines were pretreated or not with NAC (10 mM) for 3 hr and then treated with CBD (20 μ M) and BORT (3 ng/ml) alone or in combination for 2 hr. ROS production was determined by cytofluorimetric analysis. The data are represented as the mean \pm SD of at least three independent experiments. * p < 0.01 vs. vehicle; # p < 0.01 CBD-BORT vs. CBD or BORT alone; \S p < 0.01 TRPV2-transfected vs. untransfected cell lines; \S p < 0.01 NAC-treated vs. NAC untreated. (e) MM cells treated as above described were cultured for 3 days. Cell viability was determined by MTT assay. The data are represented as the mean \pm SD of at least three separate experiments. * p < 0.01 vs. vehicle; # p < 0.01 CBD-BORT vs. CBD or BORT alone; \S p < 0.01 NAC-treated vs. NAC untreated. (d–e) NAC alone treatments data were omitted, since no differences were observed compared with vehicle.

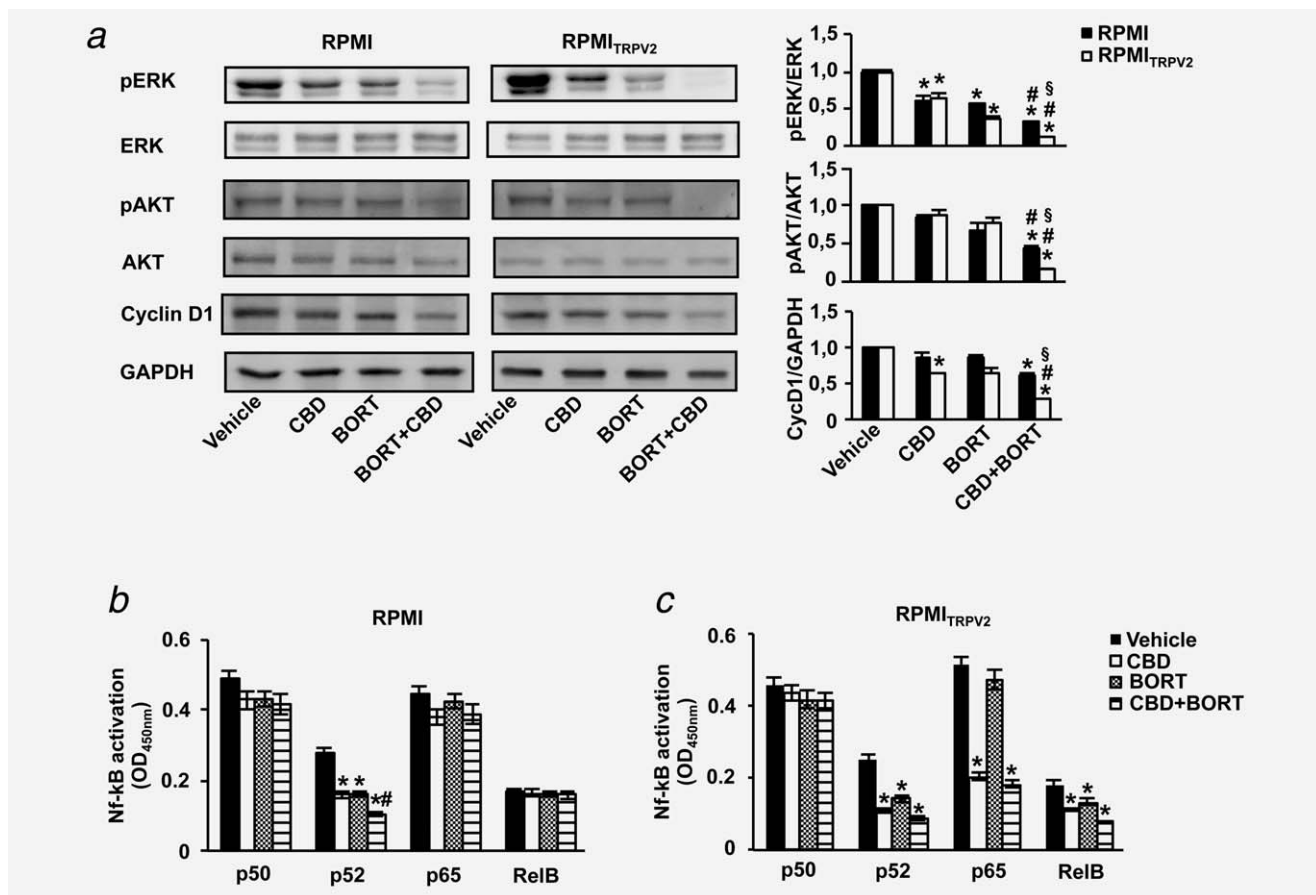


Figure 5. TRPV2 triggers the suppression of AKT and ERK activation in MM cells cotreated with CBD and BORT and increases CBD-mediated inhibition of NF- κ B canonical and alternative pathways in RPMI and RPMI_{TRPV2} cells. (a) RPMI and RPMI_{TRPV2} cells were cultured for 3 days in the presence of CBD (20 μ M) and BORT (3 ng/ml) alone or in combination. pERK, ERK, pAKT, AKT and cyclin D1 levels were analysed by Western blot. The relative protein levels were determined using GAPDH as a loading control. Blots are representative of one of three separate experiments. Bar graphs represent the mean \pm SD of at least three separate experiments. * p < 0.01 vs. vehicle; # p < 0.01 CBD-BORT vs. CBD or BORT alone; § p < 0.01 TRPV2-transfected vs. untransfected cell lines. (b,c) RPMI and RPMI_{TRPV2} cells were cultured for 3 days in the presence of CBD (20 μ M) and BORT (3 ng/ml) alone or in combination, and nuclear NF- κ B subunits were analysed by enzyme-linked immunosorbent assay. The data shown represent the mean OD \pm SD of at least three separate experiments. * p < 0.01 vs. vehicle; # p < 0.01 CBD-BORT vs. CBD or BORT alone.

effect was significantly increased upon coadministration of CBD and BORT (RPMI = 104, RPMI_{TRPV2} = 199, U266 = 133, U266_{TRPV2} = 192; p < 0.01; Figs. 4a and 4b; Supporting Information Figs. S7a and S7b). In addition, CBD, but not BORT, significantly reduced $\Delta\psi_m$, mainly in TRPV2-transfected MM cells (RPMI = 85, RPMI_{TRPV2} = 35, U266 = 80, U266_{TRPV2} = 45; p < 0.01), and this value further increased following CBD and BORT coadministration (RPMI = 74, RPMI_{TRPV2} = 28, U266 = 64, U266_{TRPV2} = 37; p < 0.01; Fig. 4c; Supporting Information Fig. S7c). Mitochondrial depolarisation was accompanied by the generation of CBD-induced reactive oxygen species (ROS) mainly in TRPV2-transfected MM cells (RPMI = 58, RPMI_{TRPV2} = 154, U266 = 76, U266_{TRPV2} = 206; p < 0.01), and this level was further increased in MM cells cotreated with CBD and BORT (RPMI = 156, RPMI_{TRPV2} = 253, U266 = 143, U266_{TRPV2} = 279; p < 0.01; Fig. 4d; Supporting Information Fig. S7d), inducing a reduction in cell viability, mainly in TRPV2-transfected cell

lines (Fig. 4e; Supporting Information Fig. S7e). To further examine the effects of BORT and CBD, the free radical scavenger NAC was used. The pretreatment with NAC 10 mM abrogated the increase in ROS generation (Fig. 4d; Supporting Information Fig. S7d) and the reduction in cell viability (Fig. 4e; Supporting Information Fig. S7e), mainly in CBD- and BORT-treated cells.

BORT and CBD abrogate activation of the AKT and ERK pathways in MM cell lines

We found that both ERK and AKT proteins were basally phosphorylated in untransfected and TRPV2-transfected MM cells (Fig. 5a; Supporting Information Fig. S8a), and CBD and BORT strongly synergised to decrease pERK levels in all MM cell lines. Similarly, CBD or BORT alone inhibited ERK activation in TRPV2-transfected and untransfected MM cells, albeit at lower levels. In addition, CBD and BORT strongly abrogated AKT phosphorylation (approximately 80%

inhibition in *TRPV2*-transfected MM cells). Finally, the effect of CBD and BORT in regulating cyclin D1 levels was evaluated. CBD alone or in combination with BORT reduced the cyclin D1 levels mainly in *TRPV2*-transfected compared with untransfected MM cells (Fig. 5a; Supporting Information Fig. S8a).

TRPV2 expression increases CBD-mediated inhibition of classical and alternative NF- κ B pathways in MM cells

We next evaluated the DNA binding activation of the p50, p65, p52 and RelB NF- κ B subunits in nuclear extracts from *TRPV2*-transfected and untransfected MM cell lines, which had been treated for 3 days with CBD or BORT alone and in combination. A reduction in p52 DNA binding activation in *TRPV2*-transfected and untransfected MM cells treated with CBD (optical density [OD]: RPMI = 0.16, RPMI_{TRPV2} = 0.11, U266 = 0.17, U266_{TRPV2} = 0.12; $p < 0.01$) and/or BORT (OD: RPMI = 0.16, RPMI_{TRPV2} = 0.14, U266 = 0.17, U266_{TRPV2} = 0.12; $p < 0.01$) was observed (Figs. 5b and 5c; Supporting Information Figs. S8b and S8c). In addition, CBD alone or in combination with BORT strongly reduced the DNA binding activation of p65 (CBD-treated OD: RPMI_{TRPV2} = 0.20, U266_{TRPV2} = 0.23; CBD plus BORT-treated OD: RPMI_{TRPV2} = 0.18, U266_{TRPV2} = 0.22; $p < 0.01$) and RelB (CBD-treated OD: RPMI_{TRPV2} = 0.11, U266_{TRPV2} = 0.12; CBD plus BORT-treated OD: RPMI_{TRPV2} = 0.07, U266_{TRPV2} = 0.09; $p < 0.01$) in *TRPV2*-transfected MM cells (Figs. 5b and 5c; Supporting Information Figs. S8b and S8c), whereas BORT alone slightly reduced only RelB (OD: RPMI_{TRPV2} = 0.13, U266_{TRPV2} = 0.14; $p < 0.01$) activation in *TRPV2*-transfected MM cells (Figs. 5b and 5c; Supporting Information Figs. S8b and S8c).

Discussion

To better define the molecular basis of MM, patient outcomes and new therapeutic targets, FISH analysis and gene expression profiling of highly purified CD138⁺ PCs have been used.^{1,5,28} *TRPV2*, which is located on 17p11.2, has been shown to regulate malignant transformation processes such as cell proliferation, survival and chemoresistance in different cancer cells and tissues,^{16–18,23} *TRPV2* gene mutations have also been identified in MM,^{19,20} although the role of *TRPV2* has not been investigated thus far.

We first evaluated the expression profile of *TRPV2* in CD138⁺ cells derived from newly diagnosed MM patients as well as RPMI and U266 MM cell lines. By flow cytometric analysis, we demonstrated the presence of two distinct CD138⁺ subpopulations according to the expression of *TRPV2* (CD138⁺*TRPV2*⁺ and CD138⁺*TRPV2*⁻) in MM samples, although deletion of 17p was not detected in the MM patients analysed. This finding strengthens the modern concept of the coexistence of genetic heterogeneity in MM cells from early stages²⁹ when only the CD138⁺*TRPV2*⁻ population exists, as observed in the RPMI and U266 MM cell lines. Thus, to mimic the *in vivo* MM phenotypes, we

transiently transfected MM cell lines with *TRPV2* cDNA to obtain *TRPV2*⁺ MM cell lines (RPMI_{TRPV2} and U266_{TRPV2} cells).

We recently reported the ability of CBD, *via* its role as a *TRPV2* agonist, to inhibit the proliferation and increase the cytotoxicity of glioma cells.¹⁷ In addition, CBD was shown to suppress proliferation and induce apoptosis in Jurkat and MOLT-4 leukaemia cells.²⁵ However, the effect of CBD in myeloma cells remained unclear. Our results are the first to show that CBD induces cytotoxicity in MM cells and that this effect was amplified in *TRPV2*-positive cells. BORT, a highly selective and reversible inhibitor of 26S proteasomes and ubiquitin-dependent proteolysis, is currently used as single agent to treat front-line and relapsed, refractory MM. In addition, the combination of various anticancer therapies has demonstrated several advantages over single-agent based strategies, particularly in overcoming drug resistance. In fact, the administration of CBD together with anticancer drugs has been shown to increase the susceptibility of cancer cells to the cytotoxic effects of drugs.^{17,23,30} We found that in MM cell lines, the coadministration of CBD and BORT (using the lowest effective dose for each drug) synergistically reduced the viability of *TRPV2*-transfected and untransfected MM cell lines. Previous findings demonstrated that both CBD than BORT acted inducing cell death in haematological cancer cells, at least in part, by generation of ROS and oxidative stress.^{25,31} Herein, we found that CBD and BORT synergistically inhibited cell growth, cell cycle arrest at the G1 phase and accumulation of cells in the subG1 phase and induced mitochondrial and ROS-dependent necrosis, mainly in *TRPV2*⁺CD138⁺ MM cells. The action of CBD is mediated by different cellular receptors, including the CB1 and CB2 receptors, *TRPV1* and *TRPV2* and PPAR γ .^{21–23,32} We found, as evaluated by the use of specific antagonists, that the effect of CBD on *TRPV2*⁻ MM cells was independent of the CB1 and CB2 receptors, TRPs and PPAR γ . Finally, our colony-forming assays established that CBD and BORT do not target CD34⁺ cells, providing an ideal strategy for developing combination therapies to eliminate MM cell populations without cytotoxic effects on haematopoietic progenitor cells.

In the BM, the mechanisms contributing to pathogenesis and chemoresistance of MM include the Ras/Raf/MEK/ERK, phosphatidylinositol 3-kinase (PI3K)-AKT and NF- κ B signalling pathways.^{33,34} In MM cells, complete blockade of pERK modulates the cell cycle by reducing cyclin D1 expression, increasing subG1 and decreasing S phase cells; moreover, ERK inhibitors showed cytotoxicity against the majority of tumour cells obtained from relapsed and refractory MM patients.³⁵ Additionally, inactivation of ERK signalling was shown to result in markedly increased DNA damage and massive cell death in MM cells.³⁶ *Cyclin D1* mRNA is frequently overexpressed in myeloma due to an IgH/*cyclin D1* translocation.³⁷ In addition, translation of *cyclin D1* is regulated by ERK and AKT in MM cell lines.^{38,39} The PI3K/AKT pathway is constitutively active in MM and shows pleiotropic

effects ranging from functional inactivation of proapoptotic BAD and cell cycle regulatory molecules, such as mammalian target of rapamycin [mTOR] and NF- κ B.⁴⁰ However, inhibition of AKT phosphorylation was less effective in MM cells where ERK phosphorylation was still evident, suggesting that combination therapy with ERK and AKT inhibitors may be more effective for MM therapy.⁴¹

BORT induces cell cycle arrest and death in MM cells *via* a plethora of mechanisms, including interference with AKT phosphorylation^{42,43} and synergism with ERK inhibitors.⁴³ Herein, we found that CBD-BORT treatment reduced ERK and AKT signals and switched off of ERK, AKT phosphorylation and cyclinD1 levels in CBD-BORT-treated MM cell lines, particularly TRPV2-positive cells. Therefore, given the role of the MEK/ERK and AKT pathways in MM, the combination of CBD-BORT may constitute a rational strategy for MM treatment.

The NF- κ B pathway is constitutively active in CD138⁺ cells derived from MM patients, and its suppression has been shown to induce MM cell death.⁴⁴ NF- κ B is activated by the classical (p50/p65) and alternative (p52/RelB) pathways. In MM patients, both pathways are activated, suggesting that classical and alternative NF- κ B signalling may both play a role in MM pathogenesis.^{10,44,45} We found that BORT inhibited p52 DNA binding activity and therefore activation of alternative pathway in MM cells expressing p52,^{45,46} as

reported previously. Furthermore, the expression of TRPV2 in MM cells not only increased the effects of CBD alone or in combination with BORT but also affected the canonical NF- κ B pathway by strongly reducing the nuclear binding activation of p65, which suggests that TRPV2 expression in MM cells specifically sensitises these cells to the effects of CBD.

In conclusion, this study demonstrated that freshly isolated PCs are heterogeneous in terms of TRPV2 expression and that TRPV2 activation may represent be a promising target to deregulate MM signalling pathways. Moreover, CBD used alone or in combination with BORT-induced necrotic death both in CD138⁺TRPV2⁺ and CD138⁺TRPV2⁻ MM cells by regulating ERK, AKT and the canonical and alternative NF- κ B pathways. Thus, these findings rationalise the putative use of CBD in combination therapy with BORT, for preclinical studies to evaluate the potential use of CBD and BORT combination as MM therapy. Moreover suggesting the possibility to use reduced BORT dose and consequently reducing adverse effects in MM patients.

Acknowledgements

This work was supported by AIL-Ancona ONLUS and the University of Camerino. M.O. received the honoraria from Janssens.

References

- Rajkumar SV. Multiple myeloma: 2011 update on diagnosis, risk-stratification, and management. *Am J Hematol* 2011;86:57–65.
- Katzel JA, Hari P, Vesole DH. Multiple myeloma: charging toward a bright future. *CA Cancer J Clin* 2007;57:301–18.
- Hideshima T, Anderson KC. Novel therapies in MM: from the aspect of preclinical studies. *Int J Hematol* 2011;94:344–54.
- Richardson PG, Sonneveld P, Schuster MW, et al. Bortezomib or high-dose dexamethasone for relapsed multiple myeloma. *N Engl J Med* 2005; 352:2487–98.
- San Miguel JF, Schlag R, Khuageva NK, et al. Bortezomib plus melphalan and prednisone for initial treatment of multiple myeloma. *N Engl J Med* 2008;359:906–17.
- Annunziata CM, Davis RE, Demchenko Y, et al. Frequent engagement of the classical and alternative NF- κ B pathways by diverse genetic abnormalities in multiple myeloma. *Cancer Cell* 2007;12:115–30.
- Keats JJ, Fonseca R, Chesi M, et al. Promiscuous mutations activate the noncanonical NF- κ B pathway in multiple myeloma. *Cancer Cell* 2007; 12:131–44.
- Ghosh S, Karin M. Missing pieces in the NF- κ B puzzle. *Cell* 2002;109 Suppl:S81–96.
- Hayden MS, Ghosh S. Shared principles in NF- κ B signaling. *Cell* 2008;132:344–62.
- Demchenko YN, Glebov OK, Zingone A, et al. Classical and/or alternative NF- κ B pathway activation in multiple myeloma. *Blood* 2010;115: 3541–52.
- Lonial S, Kaufman JL. The era of combination therapy in myeloma. *J Clin Oncol* 2012;30:2434–36.
- Munshi NC, Avet-Loiseau H. Genomics in multiple myeloma. *Clin Cancer Res* 2011;17:1234.
- Caterina MJ, Rosen TA, Tominaga M, et al. A capsaicin-receptor homologue with a high threshold for noxious heat. *Nature* 1999;398:436–41.
- Santoni G, Morelli MB, Santoni M, et al. New deals on the transcriptional and post-transcriptional regulation of TRP channel target genes during the angiogenesis of glioma. *J Exp Integr Med* 2011;1:221–34.
- Santoni G, Farfariello V, Amantini C. TRPV channels in tumor growth and progression. *Adv Exp Med Biol* 2011;704:947–67.
- Nabissi M, Morelli MB, Amantini C, et al. TRPV2 channel negatively controls glioma cell proliferation and resistance to Fas-induced apoptosis in ERK-dependent manner. *Carcinogenesis* 2010;31:794–03.
- Nabissi M, Morelli MB, Santoni M, et al. Triggering of the TRPV2 channel by cannabidiol sensitizes glioblastoma cells to cytotoxic chemotherapeutic agents. *Carcinogenesis* 2013;34: 48–57.
- Morelli MB, Nabissi M, Amantini C, et al. The transient receptor potential vanilloid-2 cation channel impairs glioblastoma stem-like cell proliferation and promotes differentiation. *Int J Cancer* 2012;131:E1067–77.
- Santoni G, Farfariello V, Liberati S, et al. The role of transient receptor potential vanilloid type-2 ion channels in innate and adaptive immune responses. *Front Immunol* 2013;4:34.
- Fabris S, Todoerti K, Mosca L, et al. Molecular and transcriptional characterization of the novel 17p11.2-p12 amplicon in multiple myeloma. *Genes Chromosomes Cancer* 2007;46:1109–18.
- Qin N, Neeper MP, Liu Y, et al. TRPV2 is activated by cannabidiol and mediates CGRP release in cultured rat dorsal root ganglion neurons. *J Neurosci* 2008;28:6231–8.
- De Petrocellis L, Ligresti A, Moriello AS, et al. Effects of cannabinoids and cannabinoid-enriched Cannabis extracts on TRP channels and endocannabinoid metabolic enzymes. *Br J Pharmacol* 2011;163:1479–94.
- Yamada T, Ueda T, Shibata Y, et al. TRPV2 activation induces apoptotic cell death in human T24 bladder cancer cells: a potential therapeutic target for bladder cancer. *Urology* 2010;76:509.e1–7.
- Mechoulam R, Peters M, Murillo-Rodriguez E, et al. Cannabidiol—recent advances. *Chem Biodivers* 2007;4:1678–92.
- McKallip RJ, Jia W, Schlomer J, et al. Cannabidiol-induced apoptosis in human leukemia cells: a novel role of cannabidiol in the regulation of p22phox and Nox4 expression. *Mol Pharmacol* 2006;70:897–08.
- Gallily R, Even-Chena T, Katzavian G, et al. Gamma-irradiation enhances apoptosis induced by cannabidiol, a non-psychoactive cannabinoid, in cultured HL-60 myeloblastic leukemia cells. *Leuk Lymphoma* 2003;44:1767–73.
- Chou TC. Theoretical basis, experimental design, and computerized simulation of synergism and antagonism in drug combination studies. *Pharmacol Rev* 2007;59:124.

28. Zhan F, Huang Y, Colla S, et al. The molecular classification of multiple myeloma. *Blood* 2006; 108:2020–28.
29. Morgan GJ, Walker BA, Davies FE. The genetic architecture of multiple myeloma. *Nat Rev Cancer* 2012;12:335–48.
30. Torres S, Lorente M, Rodríguez-Fornés F, et al. A combined preclinical therapy of cannabinoids and temozolomide against glioma. *Mol Cancer Ther* 2011;10:90–03.
31. Feng R, Oton A, Mapara MY, et al. The histone deacetylase inhibitor, PXD101, potentiates bortezomib-induced anti-multiple myeloma effect by induction of oxidative stress and DNA damage. *Br J Haematol* 2007;139:385–97.
32. De Petrocellis L, Di Marzo V. Non-CB1, non-CB2 receptors for endocannabinoids, #plant |cannabinoids, and synthetic cannabimimetics: focus on G-protein-coupled receptors and transient receptor potential channels. *J Neuroimmune Pharmacol* 2010;5:103–21.
33. Hideshima T, Catley L, Raje N, et al. Inhibition of Akt induces significant downregulation of survivin and cytotoxicity in human multiple myeloma cells. *Br J Haematol* 2007;138:783–91.
34. Li ZW, Chen H, Campbell RA, et al. NF-kappaB in the pathogenesis and treatment of multiple myeloma. *Curr Opin Hematol* 2008;15:391–99.
35. Shi L, Wang S, Zangari M, et al. Over-expression of CKS1B activates both MEK/ERK and JAK/STAT3 signaling pathways and promotes myeloma cell drug-resistance. *Oncotarget* 2010;1: 22–33.
36. Dai Y, Chen S, Pei XY, et al. Interruption of the Ras/MEK/ERK signaling cascade enhances Chk1 inhibitor-induced DNA damage in vitro and in vivo in human multiple myeloma cells. *Blood* 2008;112:2439–49.
37. Chesi M, Kuehl WM, Bergsagel PL. Recurrent immunoglobulin gene translocations identify distinct molecular subtypes of myeloma. *Ann Oncol* 2000;11:131–35.
38. Frost P, Shi Y, Hoang B, et al. Regulation of D-cyclin translation inhibition in myeloma cells treated with mammalian target of rapamycin inhibitors: rationale for combined treatment with extracellular signal-regulated kinase inhibitors and rapamycin. *Mol Cancer Ther* 2009;8:83–93.
39. Hoang B, Frost P, Shi Y, et al. Targeting TORC2 in multiple myeloma with a new mTOR kinase inhibitor. *Blood* 2010;116:4560–68.
40. Harvey RD, Lonial S. PI3 kinase/AKT pathway as a therapeutic target in multiple myeloma. *Future Oncol* 2007;3:639–47.
41. Chauhan D, Hideshima T, Anderson KC. A novel proteasome inhibitor NPI-0052 as an anticancer therapy. *Br J Cancer* 2006;95: 961–65.
42. Que W, Chen J, Chuang M, et al. Knockdown of c-Met enhances sensitivity to bortezomib in human multiple myeloma U266 cells via inhibiting Akt/mTOR activity. *APMIS* 2012;120: 195–03.
43. Kim K, Kong SY, Fulciniti M, et al. Blockade of the MEK/ERK signalling cascade by AS703026, a novel selective MEK1/2 inhibitor, induces pleiotropic anti-myeloma activity in vitro and in vivo. *Br J Haematol* 2010;149: 537–49.
44. Sen R. Control of B lymphocyte apoptosis by the transcription factor NF-kappaB. *Immunity* 2006; 25:871–83.
45. Lorch JH, Thomas TO, Schmoll HJ. Bortezomib inhibits cell-cell adhesion and cell migration and enhances epidermal growth factor receptor inhibitor-induced cell death in squamous cell cancer. *Cancer Res* 2007;67:727–34.
46. Mitsiades N, Mitsiades CS, Richardson PG, et al. The proteasome inhibitor PS-341 potentiates sensitivity of multiple myeloma cells to conventional chemotherapeutic agents: therapeutic applications. *Blood* 2003;101: 2377–80.